J Therm Anal Calorim (2016) 125:1453–1459
DOI 10.1007/s10973-016-5633-1

The influence of heat treatment on the structure and thermal properties of metallic glasses

Wirginia Pilarczyk[1] · **Adam Zarychta**[1]

Received: 30 November 2015 / Accepted: 12 June 2016 / Published online: 6 July 2016

Abstract This paper presents the structure and chosen properties of Fe-based ribbons with specified composition, after casting and heat treating. The aim of this work was to produce amorphous ribbons and study the influence of heat treatment on the structure and thermal properties before and after annealing. The base alloy ingot was prepared by induction melting of pure Fe, Co, B, Si and Nb elements in argon atmosphere. Then, the station for ultra-fast cooling of molten alloy with high vacuum pumps, designed for the production of metallic glasses in the form of ribbons by Bühler Melt Spinner SC was used. Also, the X-ray diffraction analysis system PANalytical X'Pert PRO was used. As-cast ribbons and metallic glasses after annealing were examined by differential scanning calorimetry (DSC) method, with the use of DSC822 Mettler Toledo. Annealing was done at different temperature. On the basis of obtained dependence, the glass transition temperature (T_g), onset crystallization temperature (onset—T_x) and peak crystallization temperature (peak—T_p) were determined. The supercooled liquid region (ΔT_x), specific heat and the crystallization enthalpy (ΔH) were calculated as well. The microscopic observation of cross section of ribbons was carried out by means of the Zeiss Supra 35 scanning electron microscope. Based on experimental data, the discussion on the correlation between thermal properties, structure, annealing and future application was carried out.

Keywords Metallic glasses · Amorphous materials · Thermal properties

✉ Wirginia Pilarczyk
wirginia.pilarczyk@polsl.pl

[1] Faculty of Mechanical Engineering, Silesian University of Technology, ul. Akademicka 2A, 44-100 Gliwice, Poland

Introduction

The "amorphous material" term is refer to solid state, with non-periodical atomic arrangement. The short range arrangement of atoms is the special feature of amorphous material atomic structure. However, the atomic arrangements in the atomic scale (that means distance of few diameters of atoms) are periodical. The amorphous structure of materials could be described by topological disorder and chemical disorder. The first kind of disorder is a result of dispersion of distances arrangement of atoms, because of lack of repeatable geometric packing, whereas the chemical disorder is a result of local environment of each atoms [1, 2]. On the basis of multiple tests, it can be concluded that amorphous alloys have new atomic configurations, which differ from crystalline alloys. Due to the special structure, amorphous materials have different properties from conventional crystalline alloys. Amorphous materials have been determined by many characteristic such as useful magnetic properties, good mechanical properties or unique chemical properties. Intensive development of metallic glasses and afterwards bulk metallic glasses has caused new interest on glassy metals researches [3–7].

The glass-forming ability (GFA) of an alloy reflects the physical nature of the alloy and indicates whether the alloy is a candidate for glass formation in bulk forms using conventional casting processes. GFA as a measure of the ease of vitrification is a very important parameter in designing and developing new metallic glasses in form of ribbon and bulk form with unique properties. To date, various empirical parameters have been proposed to assess the GFA of amorphous materials [8–11]. The most often used parameters are reduce glass transition temperature (T_{rg}), supercooled liquid region (ΔT_x),

$$\Delta T_x = \left(T_x - T_g\right) \quad (1)$$

critical cooling rate (R_c), stability parameter S, δ,

$$\delta = T_x/T_l - T_g \quad (2)$$

and γ, α, β indicators [4, 9, 12–14].

Inoue et al. [15] have conducted investigation of glass-forming ability, thermal stability and mechanical properties of Fe-based glassy alloys in melt-spun and cast state. As a result of the tests, it was noted that all alloys examined in the present study consist of a glassy phase in as-spun state. The glassy alloys exhibit distinct glass transition, followed by a supercooled liquid region and then crystallization. The results indicate that the ΔT_x and T_{rg} show maximum values of 50 K and 0.59, respectively. Chang et al. [16] have successfully developed a (Fe, Co, Ni)–B–Si–Nb system with high GFA, high fracture strength and good soft magnetic properties in wide composition range by the replacement of Fe by Co and Ni elements as well as the increase of B to Si concentration ration in the $(Fe_{0.75}B_{0.15}Si_{0.1})_{96}Nb_4$ glassy alloy. It has been shown that all of the alloys examined in the tested alloy system consist of a glassy phase in as-spun state, exhibiting distinct glass transition, followed by a large ΔT_x of 40–65 K. Besides, this system exhibits a high T_{rg} of 0.57–0.61.

The aim of this work was to produce amorphous ribbons with specified composition and study the structure and thermal properties after casting and heat treating. The chemical composition, precisely $Fe_{37.44}Co_{34.56}B_{19.2}Si_{4.8}Nb_{4.0}$ in form of ribbon was produced and tested for the first time. Different experimental parameters to estimate glass-forming ability of tested ribbons were calculated.

Experimental

The alloy with a nominal composition of $Fe_{37.44}Co_{34.56}B_{19.2}Si_{4.8}Nb_{4.0}$ (at.%) was prepared by induction melting of a mixture of high purity elements (99.9 % or higher) in argon atmosphere.

Rapidly, solidified alloy was prepared by the melt spinning technique (Edmund Bühler Melt Spinner SC) at different linear roller rotation speed. Figure 1 presents Bühler Melt Spinner SC station for making amorphous ribbons. The process parameters were follows:

- roller rotation speed: 10; 20; 30; 40 m s^{-1}
- vacuum: 0.735 Pa
- working pressure: 84 Pa
- casting temperature: 1392 °C
- distance between roller and crucible: 0.3 mm
- injection pressure: 42 Pa
- crucible diameter: 20 mm

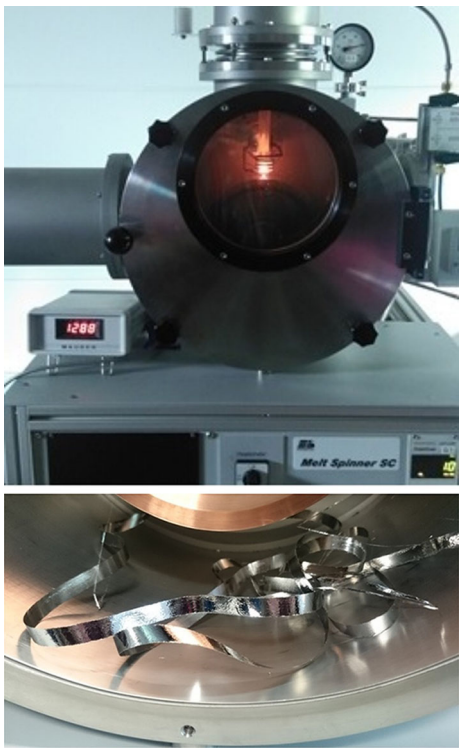

Fig. 1 Bühler melt spinner SC station for making the metallic glasses

Microstructure observations of the melt-spun ribbons were carried out on the cross sections of ribbons by means of the Zeiss Supra 35 scanning electron microscope equipped with a chemical composition analysis detector EDS by Oxford.

X-ray diffraction studies by means of PANalytical X'Pert PRO diffraction system which uses filtered radiation from the lamp with cobalt anode, with a voltage of 40 kV and heater current of 30 mA were carried out.

The study of crystallization process by differential scanning calorimetry method with the use of differential scanning calorimeter DSC852 Mettler-Tolledo (Switzerland) was carried out. The sample was analysed in a temperature range of 25–700 °C. The heating rate was 40 °C min^{-1}. Analyses were conducted under nitrogen atmosphere (flow of reaction gas 80 mL min^{-1}) in open 70 μL alumina crucibles.

The amorphous ribbons were heated at a temperature of 873 and 973 K.

Results and discussion

In this article, amorphous ribbons were obtained with the use of different critical cooling speed. The critical cooling speed was the main parameter which was changing during the ribbons production process. This was done by changing

the rotation speed of the roller. The following rotations of the copper roller were used: 10, 20, 30 and 40 m s^{-1}.

The X-ray diffraction investigations revealed that all studied as-cast ribbons were amorphous. Figure 2 presents set of diffraction patterns of tested ribbons, which were produced with different rotary speed of the roller. The XRD patterns show broad hallo diffraction patterns, which indicate the amorphous nature of obtained metallic glasses (Fig. 2a, b). The amorphous–crystalline character of analysed samples is presented in Fig. 2c, d), and crystalline phases were revealed in Fig. 2e.

To study and to confirm amorphous character of produced ribbons, the microscopic observation of the fracture morphology was carried out. The appearance of the fracture surface of the investigated samples in a form of ribbon was investigated by SEM with different magnifications. Figure 3 presents SEM images of as-cast glassy ribbons which were produced with different rotary of copper roller. Each and every fracture surface appears to consist of two

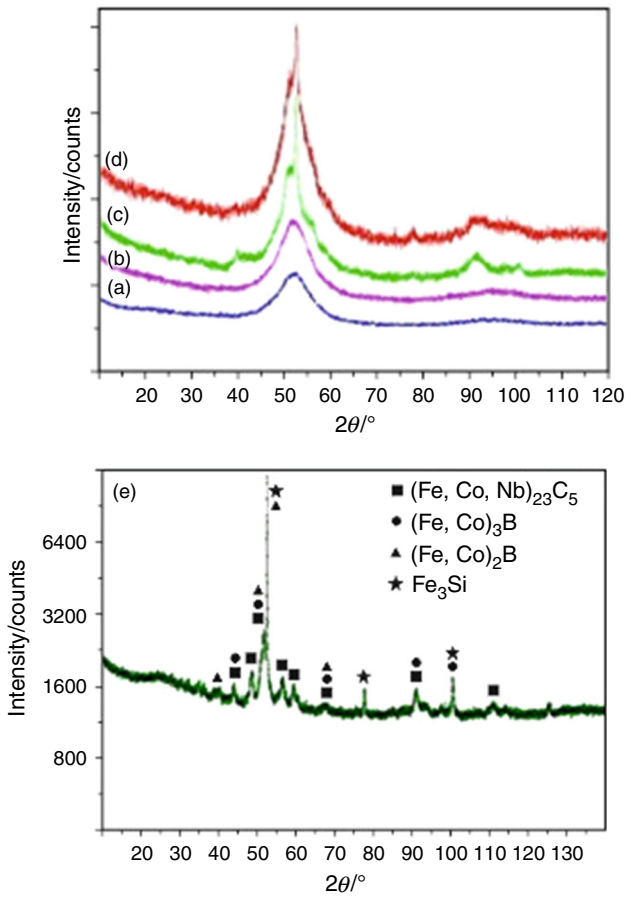

Fig. 2 X-ray diffraction patterns of $Fe_{37.44}Co_{34.56}B_{19.2}Si_{4.8}Nb_{4.0}$ glassy ribbons in as-cast state *a* rotary of copper roller: 20 m s^{-1}, as-cast state; *b* rotary of copper roller: 20 m s^{-1}, 873 K; *c* rotary of copper roller: 30 m s^{-1}, as-cast state; *d* rotary of copper roller: 30 m s^{-1}, 873 K and *e* after annealing at 973 K

different fracture zones. The fracture could be classified as mixed type with indicated zones containing the river and shell patterns and smooth areas. These patterns are characteristic for metallic glassy alloys. Morphology of fracture surface is changing from smooth fracture inside with narrow dense veins pattern in surface having contact with the copper roller during casting to fine (shell) chevron pattern in surface freely solidified (shining surface).

Figure 4 shows main view of ribbon with different morphology, smooth fracture with narrow dense veins pattern. The fracture surface of ribbons samples consists of two different zones, which inform about different amorphous structures of the treated samples and crystalline phases.

The alloy was also checked with EDS equipment to identify chemical composition of chosen areas. Chemical analysis of these areas shows the presence of exclusively Fe, Co, Si and Nb elements, which confirm chemical purity of obtained amorphous ribbons. Melting and casting process had not an influence on the purity and on chemical composition of produced samples. The curve of the X-ray dispersive energy of tested alloy is presented in Fig. 5.

The DSC curves measured on amorphous ribbons produced with the use of 10, 20, 30 and 40 m s-1 roller rotation speed in as-cast state for studied $Fe_{37.44}Co_{34.56}B_{19.2}Si_{4.8}Nb_{4.0}$ metallic glasses are shown in Fig. 6.

The distinct exothermic peak describing crystallization process of studied glassy alloy is observed for every curve. The one stage crystallization process was observed for examined ribbons. The DSC curve obtained for sample produced with at least roller rotation speed 10 m/s informs that exothermic effect includes glass transition temperature $T_g = 822$ K, onset crystallization temperature at value of $T_x = 868$ K and peak crystallization temperature at $T_p = 880$ K. The width of ΔT_x is 46 K, indicating that the Fe-based alloy possesses a sufficient stability of the supercooled liquid state. Result of DSC investigation for ribbon produced with at least largest roller rotation speed 40 m s^{-1} allows to determine glass transition temperature $T_g = 828$ K, onset crystallization temperature at value of $T_x = 869$ K and peak crystallization temperature at $T_p = 882$ K. The width of ΔT_x equals 41 K. In scientist's opinion, the width of supercooled liquid region is a very good GFA measure. From the analysis of the literature and obtained data, it can be concluded that when range of temperature ΔT_x is larger, GFA is higher. ΔT_x criterion is acknowledged through researchers in this field of science [2, 9].

Results of DSC investigations exhibited that crystallization temperature peak of sample one is smaller than the crystallization temperature peak of remained amorphous samples. The crystallization enthalpy is 61 J g^{-1} for the ribbon produced with the use of 40 m s^{-1} of roller rotation

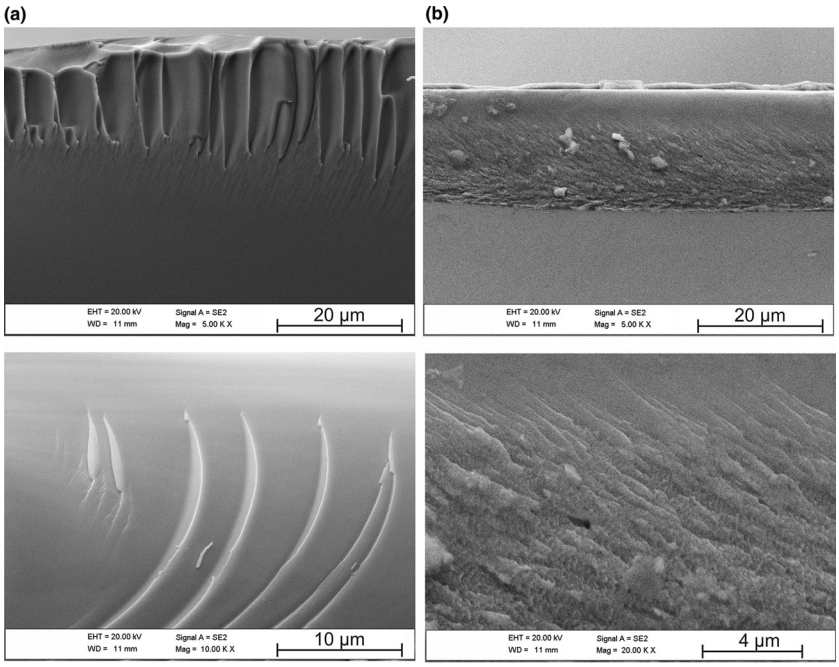

Fig. 3 Fracture surface images of Fe–Co–B–Si–Nb ribbons obtained by the use of velocity of roller **a** 20 m s^{-1} and **b** 40 m s^{-1} and after decohesion

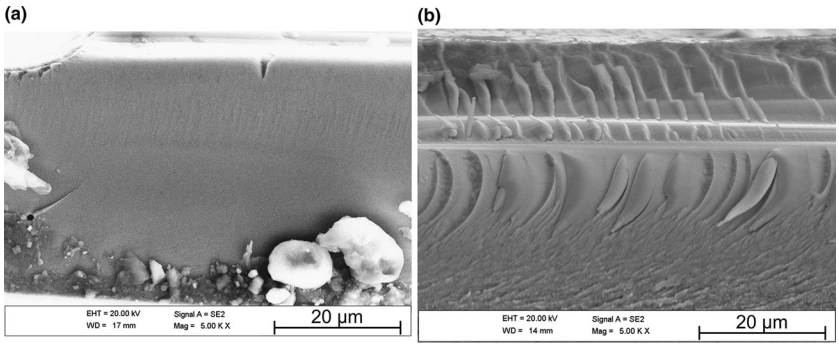

Fig. 4 Fracture surface images of Fe–Co–B–Si–Nb ribbons obtained by the use of the roller rotation speed **a** 20 m s^{-1}, annealing at 873 K and after decohesion; **b** 20 m s^{-1}, annealing at 973 K and after decohesion

speed and 47 J g^{-1} for the ribbon produced with the use of 20 m s^{-1} roller rotation speed, indicating that the amount of heat released from the system is much bigger in the case of fourth sample.

To present behaviour of metallic glasses during heat treatment, DSC curves were set and analysed. To compare DSC curves shape, the results of DSC ribbons measurement after annealing process at 873 K and after annealing at 973 K were placed in this work and were presented in Figs. 7a, b.

The samples heat treated (annealed) for an hour at the 873 K temperature have broaden and accentuate DSC line. However, it is impossible to determine characteristics exothermal or endothermal peaks basing on experimental data received from the examinations. Annealing process in the temperature close to onset crystallization temperature at value of 868, 871, 870 and 869 K results in appearing partial crystallization of tested alloy. The same situation was confirmed thanks to X-ray diffraction analysis.

X-ray rotating-crystal pattern of a chosen amorphous ribbons presents a broaden line curve in a range of 45–60 Theta with small peaks related with precipitation processes of: $(Fe, Co)_2B$, $(Fe, Co)_3B$, $(Fe, Co)_{23}B_6$ and Fe_3Si phases.

DSC curves of 1.5 h annealed ribbons at 973 K represent the straight line, what confirms that the glassy state was transformed to full entire crystallographic structure.

The characteristic crystallization temperature obtained from DSC curves is connected with thermal properties and glass-forming ability of studied metallic glass in as-cast state. The thermal stability temperatures: glass transition temperature (T_g), onset crystallization temperature (T_x), crystallization peak temperature (T_p), crystallization enthalpy and calculated glass-forming ability parameters of studied ribbons, are listed in Tables 1 and 2. Table 2 also shows reduced glass transition temperature (T_{rg}), supercooled liquid region (ΔT_x) and calculated glass-forming ability parameters: α, β, γ, δ and S parameter.

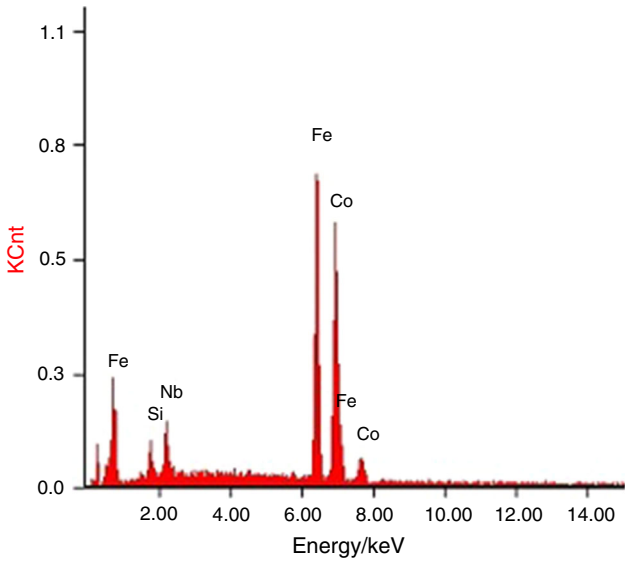

Fig. 5 EDS microanalysis of the tested metallic glasses (area from Fig. 3a)

The selected thermal stability and the glass-forming parameters: α, β, γ and S, are sufficient high for all tested samples. The calculated indicators: T_{rg}, ΔT_x, α, β, γ, differ slightly (range of 0.001). Very small differences can be caused by the way of sample preparation for testing and by complicated production process.

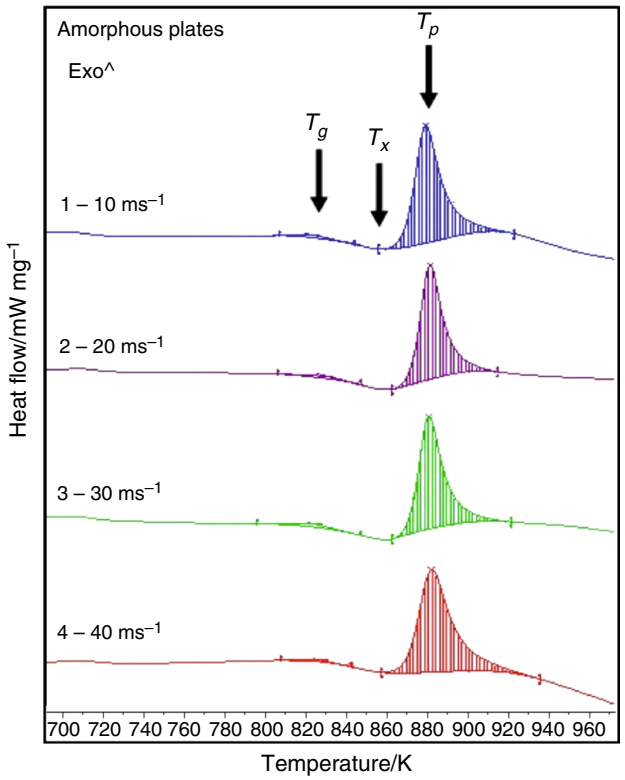

Fig. 6 DSC curves of $Fe_{37.44}Co_{34.56}B_{19.2}Si_{4.8}Nb_{4.0}$ alloy in as-cast state in form of ribbons

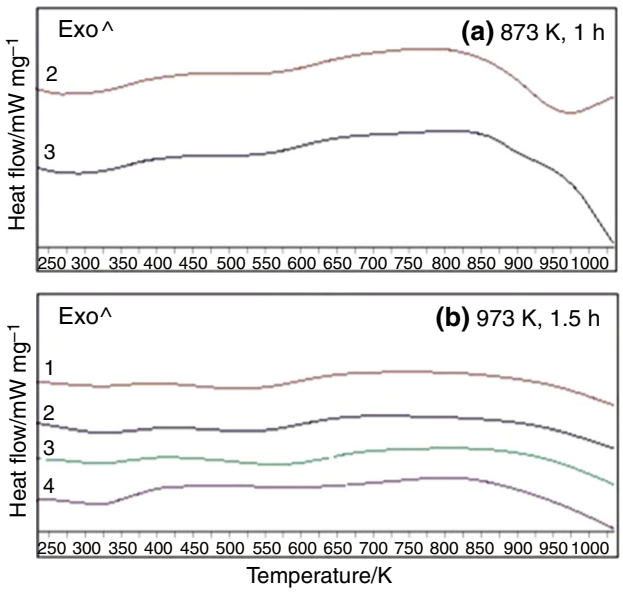

Fig. 7 DSC curves of Fe–Co–B–Si–Nb ribbons after annealing at 873 K for 1 h (**a**) and 973 K for 1.5 h (**b**)

Glass transition temperature T_g, onset crystallization temperature T_x, peak crystallization temperature and the calculated GFA parameters indicated that the insignificant best glass-forming ability have $Fe_{37.44}Co_{34.56}B_{19.2}Si_{4.8}Nb_4$ ribbons.

Obtained indicators values are not related with manufacture parameters process.

The tests results confirmed that structure of obtained ribbons are amorphous. Metallic glasses which were produced with different rotation speed of a copper roller have higher density than crystalline materials. The difference in the density is a result of free volumes, which have been formed during cooling of molten alloy. The free volumes are responsible for temperature and time instabilities of metallic glasses.

To confirm the existence of amorphous phase and to investigate the temperature influence on obtained metallic glasses structure, annealing process (in two different temperatures: 873 K and 973 K) was done. One hour

Table 1 Thermal properties of as-cast ribbons and after annealing

	Roller rotation speed/m s^{-1}	T_g/K	T_x/K	T_p/K	ΔH/J g^{-1}
1	10	822	868	880	57
2	20	829	871	882	47
3	30	824	870	882	50
4	40	828	869	882	61
5	Annealing at 873 K	–	–	–	–
6	Annealing at 973 K	–	–	–	–

Table 2 Calculated glass-forming ability parameters of as-cast ribbons and after annealing

	Roller rotation speed/m s-1	T_{rg}	ΔT_x	α	β	Γ	δ	S
1	10	0.5879	46	0.6208	1.6438	0.3909	1.5069	0.6715
2	20	0.5929	42	0.6230	1.6435	0.3911	1.5307	0.5572
3	30	0.5894	46	0.6223	1,6452	0.3915	1.5156	0.6699
4	40	0.5922	41	0.6216	1.6417	0.3903	1.5245	0.6437
5	Annealing at 873 K	–	–	–	–	–	–	–
6	Annealing at 973 K	–	–	–	–	–	–	–

annealing process, in the temperature 873 K, is responsible for partially crystallized structure of tested ribbons, while annealing process in a higher temperature (973 K) for 1.5 h transformed tested metallic glasses to full entire crystallographic structure.

Realized crystallization process can be investigated by many experimental methods, which can also provide an information to understand the influence of heat activation microstructure changes (like structural relaxation, nanocrystallization or crystallization) on structure and properties. The study of crystallization process plays a meaningful role in understanding the mechanism of phase transformations from equilibrium state, the thermal stability of metallic glasses and for producing controlled microstructure [5]. Since last decades, a lot of works have been devoted to metallic glass crystallization. However, in the opinion of Wang et al. [17], a proper understanding for the thermal stability against crystallization of the metallic glasses is still lacking. According to the literature data and tests results, in general, scheme of crystallization process of Fe–Co–B–Si–Nb system alloy in a form of ribbon obtained with different cooling rates is as follows: at the initial stage of crystallization process, metallic elements and their solutions are formed. When the crystallization process is more advanced, the temperature increase and/or the time lengthen and borides of metals and intermetallic phases are formed. As a results of numerous tests [18, 19], improving of magnetic properties of metallic glasses is a result of a formation of nanocrystalline phases. What is more, the enhancement of magnetic permeability could also be explained by decrease of magnetostriction constant and annealing [20].

Conclusions

On the basis of the investigations into the relationship between structure, thermal properties and heat treatment processes, it can be concluded that tested Fe-based amorphous alloy in form of ribbons has amorphous structure with sufficient glass-forming ability.

Moreover, 1 h annealing process, in the temperature 873 K, creates partially crystallized structure, whereas annealing process in a higher temperature (973 K) for 1.5 h forms crystallographic structure (Fe_2B, $(Fe,Co)_{23}B_6$, Fe_3B and Fe_3Si). Obtained investigation results are complementary.

Controlled crystallization of metallic glasses enables nanocrystalline materials manufacturing with much better (for example magnetic) properties than amorphous or crystalline alloys. Thermal properties and microscopic structure investigations enable proper selection of manufacturing parameters (critical cooling speed), controlling of a needed material structure (amorphous or crystalline) and proper choice of (annealing) heat treatment parameters—time and temperature.

Acknowledgements This project was funded by the National Science Centre allocated on the basis of the decision number DEC-2011/01/D/ST8/07327.

References

1. Zallen R. Physics of amorphous materials. Warszawa: PWN Warsaw; 1994.
2. Suryanarayana C, Inoue A. Bulk metallic glasses. Boca Raton: CRC Press, Taylor & Francis Group; 2011.
3. Inoue A, Takeuchi A. Recent progress in bulk glassy, nanoquasicrystalline and nanocrystalline alloys. Mat Sci Eng A Struct. 2004. doi:10.1016/j.msea.2003.10.159.
4. Pilarczyk W. Preparation and characterization of Zr-based bulk metallic glasses in form of plate. J Alloys Compd. 2014. doi:10.1016/j.jallcom.2014.01.037.
5. Hirata A, Hirotsu Y, Amiya K, Nishiyama N, Inoue A. Nanocrystallization of complex $Fe_{23}B_6$-type structure in glassy Fe–Co–B–Si–Nb alloy. Intermetallics. 2008. doi:10.1016/j.intermet.2007.11.006.

6. Gębara P, Pawlik P, Michalski B, Wysłocki JJ. Measurements of magnetocaloric effect in LaFe11.14Co0.66Si1.2–xAlx (x = 0.1, 0.2, 0.3) alloys. Acta Phys Pol, A. 2015. doi:10.12693/APhysPolA.127.576.
7. Lipiński T. Double modification of $AlSi_9Mg$ alloy with boron, titanium and strontium. Arch Metall Mater. 2015. doi:10.1515/amm-2015-0394.
8. Chen Q, Shen J, Zhang D, Fan H, Sun J, McCartney DG. A new criterion for evaluating the glass-forming ability of bulk metallic glasses. Mater Sci Eng A Struct. 2006. doi:10.1016/j.msea.2006.06.053.
9. Shen J, Zou J, Ye L, Lu ZP, Xing DW, Yan M, Sun JF. Glass-forming ability and thermal stability of a new bulk metallic glass in the quaternary Zr–Cu–Ni–Al system. J Non Cryst Solids. 2005. doi:10.1016/j.jnoncrysol.2005.07.009.
10. Singh PK, Dubey KS. Thermodynamical analysis of the glass-forming ability of bulk metallic glasses. J Therm Anal Calorim. 2012. doi:10.1007/s10973-011-2106-4.
11. Wu J, Pan Y, Pi J. On non-isothermal kinetics of two Cu-based bulk metallic glasses. J Therm Anal Calorim. 2014. doi:10.1007/s10973-013-3288-8.
12. Pilarczyk W. The study of glass forming ability of Fe-based alloy for welding processes. J Achiev Mater Manuf Eng. 2012;52(2):83–90.
13. Kozieł T, Latuch J, Zielińska-Lipiec A. Structure of the amorphous-crystalline $Fe_{66}Cu_6B_{19}Si_5Nb_4$. Arch Metall Mater. 2015. doi:10.2478/amm-2013-0044.
14. Patel AT, Shevde HR, Pratap A. Thermodynamics of Zr52.5Cu17.9Ni14.6Al10Ti5 bulk metallic glass forming alloy. J Therm Anal Calorim. 2012. doi:10.1007/s10973-011-1591-9.
15. Inoue A, Shen BL, Chang CT. Super-high strength of over 4000 MPa for Fe-based bulk glassy alloys in $[(Fe_{1-x}Co_x)_{0.75}B_{0.2}Si_{0.5}]_{96}Nb_4$ system. Acta Mater. 2004. doi:10.1016/j.actamat.2004.05.022.
16. Chang Ch, Shen B, Inoue A. Synthesis of bulk glassy alloys in the (Fe, Co, Ni)–B–Si–Nb system. Mater Sci Eng A Struct. 2007. doi:10.1016/j.msea.2006.02.253.
17. Wang WH. Crystallization of ZrTiCuNiBe bulk metallic glasses. Ann Chim Sci Mater. 2002. doi:10.1016/S0151-9107(02)80050-2.
18. Kulik T. Nanocrystallization of metallic glasses. J Non Cryst Solids. 2001. doi:10.1016/S0022-3093(01)00627-5.
19. Kronmüller H. Micromagnetism and microstructure of amorphous alloys. J Appl Phys. 1981. doi:10.1063/1.329552.
20. Kronmüller H. Magnetization process and the microstructure in amorphous metals. J Phys Colloq. 1980. doi:10.1051/jphyscol:19808156.